Interacting Weyl Semimetals: Characterization via the Topological Hamiltonian and its Breakdown

William Witczak-Krempa,[1] Michael Knap,[2,3] and Dmitry Abanin[1]

[1]*Perimeter Institute for Theoretical Physics, Waterloo, Ontario N2L 2Y5, Canada*
[2]*Department of Physics, Harvard University, Cambridge, Massachusetts 02138, USA*
[3]*ITAMP, Harvard-Smithsonian Center for Astrophysics, Cambridge, Massachusetts 02138, USA*
(Received 12 June 2014; published 25 September 2014)

Weyl semimetals (WSMs) constitute a 3D phase with linearly dispersing Weyl excitations at low energy, which lead to unusual electrodynamic responses and open Fermi arcs on boundaries. We derive a simple criterion to identify and characterize WSMs in an interacting setting using the exact electronic Green's function at zero frequency, which defines a topological Bloch Hamiltonian. We apply this criterion by numerically analyzing, via cluster and other methods, interacting lattice models with and without time-reversal symmetry. We identify various mechanisms for how interactions move and renormalize Weyl fermions. Our methods remain valid in the presence of long-ranged Coulomb repulsion. Finally, we introduce a WSM-like phase for which our criterion breaks down due to fractionalization: the charge-carrying Weyl quasiparticles are orthogonal to the electron.

The emergence of (quasi)relativistic excitations in quantum condensed matter has stimulated much theoretical and experimental research, especially following the discoveries of graphene [1,2] and 3D topological insulators [3,4], both of which host 2D massless Dirac fermions. More recently, a 3D analog of graphene, the Weyl semimetal (WSM), has piqued physicists' curiosity, partially due to its potential for realization in transition metal oxides with strong interactions and spin-orbit coupling [5–8], or heterostructures [9]. Such a phase has stable massless Weyl quasiparticles, which can be viewed as half-Dirac fermions. These lead to unique open Fermi arc surface states [5] and electromagnetic responses [10–18]. Such properties rely on the topological nature of the Weyl points [19], which are monopoles of the noninteracting Berry curvature. As WSMs naturally arise in interacting lattice models [8,13,14], it is important to characterize them without relying on free-electron or field-theoretic approaches [20–23], neither of which is sufficient to provide accurate predictions for most realistic systems. Moreover, an efficient method for searching for Weyl points in the interacting setting is desired because they generally occur at incommensurate points in the Brillouin zone (BZ), often due to spontaneous symmetry breaking.

We provide a simple criterion to identify and characterize WSMs in the quantum many-body setting based on the electronic lattice Green's function. Specifically, we use an effective Bloch Hamiltonian (dubbed "topological Hamiltonian" [24]) defined from the zero-frequency many-body Green's function, and argue that its eigenstates retain the Berry phase properties of the Weyl nodes. This allows for the extraction of the nontrivial surface states [5] and anomalous quantum Hall (AQH) response [11,12] of

interacting WSMs. We apply our results in conjunction with cluster perturbation theory [26] to study the physics of two interacting lattice models for WSMs, unraveling diverse interaction effects on the renormalization of the Weyl points. We also discuss the effects of long-range Coulomb repulsion which marginally destroys the quasiparticles [27], and argue that our approach remains valid in that case. Finally, we provide an instance where such methods break down due to a simple fractionalization into an orthogonal [28] WSM. Our analysis naturally relates to previous works that characterized interacting topological insulators [20,29–35] by means of the many-body Green's function and associated Berry curvature, but differs in the sense that we study gapless systems.

Characterizing interacting Weyl semimetals.— Noninteracting WSMs have a Fermi surface consisting of a finite number of points in the BZ, at which 2 bands meet linearly. Each such Weyl point can be identified with a hedgehog singularity of the Berry curvature, $\nabla \times \boldsymbol{a}(\boldsymbol{k})$, i.e., a monopole of this k space "magnetic" field. Here, $\boldsymbol{a}$ is the Berry connection defined via the occupied Bloch states. Knowledge of this monopole structure naturally leads to a description of the unusual open Fermi arc surface states [5], and AQH response [11,12]. In the presence of interactions that inevitably arise in realistic systems, the above band structure description no longer applies. However, we demonstrate that the essential features of the WSM remain robust, and can be understood in terms of the zero-frequency Green's function.

We focus on short range interactions, while the effects of the long-ranged Coulomb repulsion are discussed towards the end. The central tool in our analysis is the imaginary-frequency Green's function, $G(i\omega, \boldsymbol{k})$. It is a matrix in spin,

orbital, or sublattice space, and k belongs to the BZ of the lattice of the interacting system. A key observation is that one can define a many-body Berry connection $\mathcal{A}(k)$, and associated Berry curvature $\nabla \times \mathcal{A}$, using the zero-frequency Green's function. One begins by defining the so-called topological Hamiltonian,

$$\mathcal{H}_t(k) = -G(0,k)^{-1} = \mathcal{H}(k) + \Sigma(0,k), \qquad (1)$$

where $\mathcal{H}$ is the Bloch Hamiltonian of the noninteracting system, while $\Sigma(i\omega,k)$ is the exact self-energy matrix. $\mathcal{H}_t$ plays the role of an effective Bloch Hamiltonian: its eigenstates can be loosely viewed as substitutes of the Bloch states of the noninteracting system. The many-body Berry connection can then be introduced in exact analogy with noninteracting systems: $\mathcal{A}(k) = -i\sum_{Rzeros}\langle nk|\nabla|nk\rangle$, where $\mathcal{H}_t(k)|nk\rangle = \tilde{\xi}_n(k)|nk\rangle$ and $\{\tilde{\xi}_n(k)\}$ defines the band structure of $\mathcal{H}_t$. R zero [29] signifies an eigenstate with $\tilde{\xi}_n(k) \leq 0$. In the noninteracting limit, R zeros reduce to occupied states, and $\mathcal{A}$ to a. We now argue that Weyl points of the interacting system can then be identified with monopoles of $\nabla \times \mathcal{A}$ (analogously for higher charge monopoles [36]). An equivalent but more practical criterion follows: an interacting system is a WSM if the band structure of the topological Hamiltonian $\mathcal{H}_t$ has Weyl nodes at the Fermi level, which identify the Weyl nodes of the interacting system.

To understand the above criterion, let us consider a noninteracting WSM for which short-ranged interactions (attractive or repulsive) are adiabatically turned on. The latter are irrelevant in the renormalization group sense, i.e., at low energy, and one thus obtains a *Weyl liquid*, where excitations have an infinite lifetime only on the Fermi surface, i.e., at the Weyl nodes. By adiabacity, the monopole structure of the noninteracting Green's function cannot be destroyed in the Weyl liquid. The many-body Berry connection $\mathcal{A}$ captures the monopole of Berry flux [21] associated with the Weyl quasiparticles. This relates to Haldane's statement [11] about using the Berry curvature of the quasiparticles of a Fermi liquid to determine its AQH response [which translates to our expression for the latter, Eq. (2), being valid in that case], as one can approach a Weyl liquid from its parent Fermi liquid by tuning the doping.

We now support the above arguments by deriving the AQH response of a WSM in terms of the generalized Berry curvature $\mathcal{A}$. We proceed by evaluating the many-body Chern number for 2D surfaces away from the Weyl points in the BZ [21]. More precisely, we will show that the anomalous part of the Hall conductivity reads

$$\sigma_{ab} = \frac{e^2}{2\pi h}\epsilon_{abc}K^c, \qquad K = \int_{BZ}\frac{d^3k}{2\pi}\nabla \times \mathcal{A}(k), \quad (2)$$

where ϵ_{abc} is the Levi-Civita tensor. Equation (2) generalizes the noninteracting formula [11], and can be collapsed

to Fermi surface data $K = \sum_m q_m k_m$, where k_m is a Weyl node of the interacting system, and $q_m = \pm 1$ its monopole charge. Equation (2) can be deduced by starting with the frequency-dependent Green's function. For simplicity, we consider a fixed k_x away from the Fermi surface of the interacting WSM. It follows that $G(i\omega,k)$ defines a gapped 2D Green's function in the $k_{y,z}$ plane. We can compute the many-body Chern number associated with G at fixed k_x [37,38]:

$$C_x(k_x) = \int\frac{d\omega dk_{y,z}}{24\pi^2}\epsilon_{\mu\nu\rho x}\text{Tr}G\partial_\mu G^{-1}G\partial_\nu G^{-1}G\partial_\rho G^{-1}. \quad (3)$$

The x component of the anomalous Hall vector is then the integral over the Chern number $K_x = \int dk_x C_x(k_x)$. We note that this latter expression agrees with the so-called Adler-Bell-Jackiw anomaly coefficient of the current correlator (see Supplemental Material [39]). Now, to recover Eq. (2), we adiabatically deform the interacting Green's function into the topological Green's function, $G_t(i\omega,k)^{-1} = i\omega - \mathcal{H}_t(k)$, via the interpolation $g_\lambda(i\omega,k) = (1-\lambda)G(i\omega,k) + \lambda G_t(i\omega,k)$, $0 \leq \lambda \leq 1$. Indeed, for any slice away from the Fermi surface, the gap of g_λ remains open during the protocol since $g_\lambda(0,k) = G(0,k)$ for all λ. Further, $g_\lambda(i\omega,k)$ does not have zero eigenvalues [30]. Thus, the many-body Chern number cannot change as λ varies from 0 to 1, being a topological index, and we can use $g_{\lambda=1} = G_t(i\omega,k)$ to compute C_x. The frequency integral then yields Eq. (2) [39].

Using topological Hamiltonians numerically.—We study two lattice models of interacting WSMs numerically to show the usefulness of the topological Hamiltonian approach. We identify and explain the motion and renormalization of the Weyl points as a function of the interaction strength. We consider Hubbard models

$$H = H_0 + U\sum_r n_{r,\uparrow}n_{r,\downarrow} - \mu\sum_{r,\sigma}n_{r,\sigma}, \qquad (4)$$

where H_0 is a tight-binding hopping Hamiltonian of spin-1/2 electrons, which are created at site r by $c_{r,\sigma}^\dagger$, and their number density per spin projection is $n_{r,\sigma} = c_{r,\sigma}^\dagger c_{r,\sigma}$. U is the Hubbard interaction parameter; we consider both the attractive and repulsive cases. We study models that are defined on the cubic lattice, have particle-hole symmetry and are WSMs at the noninteracting level, and fix the chemical potential at the nodes, $\mu = U/2$.

Model I breaks time reversal and is defined by [12]

$$\begin{aligned} H_0 = \sum_k c_k^\dagger[\{2t(\cos k_x - \cos k_0) \\ + m(2 - \cos k_y - \cos k_z)\}\sigma_x + 2t\sin k_y\sigma_y \\ + 2t\sin k_z\sigma_z]c_k, \end{aligned} \qquad (5)$$

where the spacing of the cubic lattice has been set to unity, and the fermion operators are vectors in spin space. The Pauli matrices σ_a act on the latter. Below we set $t = 1$. Depending on the parameters k_0 and m, H_0 can have 2, 6, or 8 Weyl nodes. We focus on the regime where it only has 2 nodes, located on the BZ boundary at $\boldsymbol{k} = \pm(k_0, 0, 0)$. See Fig. 1(a) for the $U = 0$ band structure (recall that in that limit $\mathcal{H}_t = \mathcal{H}$). The anomalous Hall vector is thus given by $\boldsymbol{K} = 2k_0\hat{x}$, i.e., $\sigma_{yz} = (e^2/2\pi h)2k_0$.

We now turn to the study of the interacting Hamiltonian using cluster perturbation theory [26] (CPT). This method, which is related to dynamical mean field theory, allows for an efficient numerical analysis. In essence, one first decomposes the periodic system into clusters with N_c sites. Exact diagonalization is used to obtain the exact cluster Green's function. The Green's function of the lattice system is then obtained via strong-coupling perturbation theory. CPT becomes exact in the limit $U \to 0$ and at strong coupling, $U \to \infty$; it is controlled in the sense that convergence can be monitored with increasing the cluster size. We emphasize that it is not perturbative in U. See Supplemental Material [39] for more details.

CPT allows a direct evaluation of the topological Hamiltonian $\mathcal{H}_t$, so that we can easily track the location of the Weyl points of the interacting system as a function of U. The results we present are for clusters of size $N_c = 2^3$, at which point reasonable convergence with N_c has been

achieved [39]. A further increase of N_c would not affect our conclusions. We set $m = 3/2$, and $k_0 = 3\pi/8$. The positive band of the topological Hamiltonian is shown in Fig. 1(a) for a cut through the BZ and for different U values. With increasing $U > 0$, the Weyl points move to larger magnitude of the wave vector. This directly corresponds to an increase of the Hall conductivity σ_{yz}, Eq. (2), as shown in Fig. 1(b). The red circles are evaluated numerically with CPT. We also show the analytic strong coupling result (perturbative in $1/U$ [39]), i.e., for single-site clusters, which captures the overall trend. For attractive interactions $U < 0$, the trend is opposite: the Weyl points move towards $\boldsymbol{k} = 0$. One can understand this heuristically: a positive (negative) U enhances (reduces) the ferromagnetic moment $\langle c_r^\dagger \sigma_x c_r \rangle$ (already present at $U = 0$), thus, enhancing (reducing) the Hall conductivity. A crude estimate of this effect can be obtained using mean field theory [39] as shown in Fig. 1(b).

In studying the Weyl points and AQH response of the many-body system, the topological Hamiltonian allowed a streamlined analysis by circumventing the need for the full frequency-dependent Green's function. We now discuss some of the properties arising from the latter but not captured by $\mathcal{H}_t$. The spectral function $A(\omega, \boldsymbol{k}) = -\mathrm{Tr}\,\mathrm{Im}G_R(\omega + i0^+, \boldsymbol{k})/\pi$ obtained using CPT for $U \geq 0$ is shown in Fig. 2. The linearly dispersing Weyl modes can clearly be seen. In the interacting WSM only the excitations at the Weyl points remain sharp. The scattering rate of an excitation with momentum exactly at a Weyl point and with small frequency vanishes like $|\omega|^5$, as can be obtained perturbatively [39]. This is smaller than the Fermi liquid result ω^2, owing to the vanishing density of states at the Fermi level in a WSM. As in a FL, the weight of the quasiparticles Z will be reduced with increasing interactions. (When the Weyl nodes are related by symmetry they share the same Z, which is the case in this work.) The result is plotted in Fig. 2(c), and as expected behaves as $Z \approx 1 - \alpha U^2$ at small U, $\alpha > 0$.

We introduce a new model which, in contrast to model I, preserves TRS but not inversion, and as such is a representative of the second family of WSMs. We show that the influence of interactions on the motion of the Weyl points has an altogether different physical origin as compared to model I, but a connection can be made by interchanging the role of magnetic and charge orders. The tight-binding Hamiltonian of model II reads

$$H_0 = 2t \sum_{\boldsymbol{k}, b=x,y,z} c_{\boldsymbol{k}}^\dagger \sigma_b \sin k_b c_{\boldsymbol{k}} + \epsilon H_{\mathrm{cdw}}, \qquad (6)$$

where H_{cdw} corresponds to a $(\pi, \pi, 0)$ charge density wave (CDW) on the cubic lattice where the chemical potential is staggered by $\pm\epsilon$ in a checkerboard fashion in the xy plane. When $\epsilon = 0$, we do not expect the 8 Weyl points to move under the effect of interactions (modulo possible
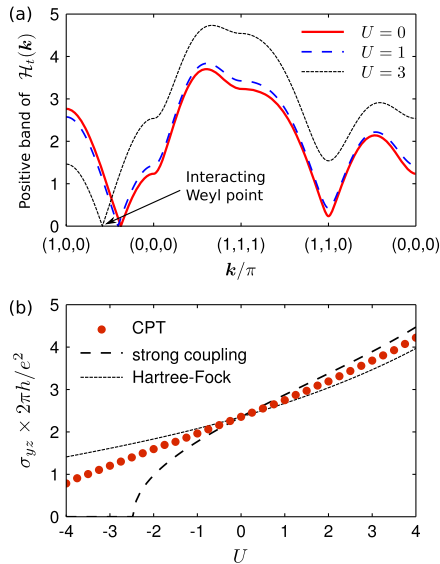

FIG. 1 (color online). (a) Positive band of the topological Hamiltonian $\mathcal{H}_t = -G(0, \boldsymbol{k})^{-1}$ of model I with varying interaction strength U along a cut through the BZ. (b) The Weyl points move with varying U, altering the Hall conductivity σ_{yz}. Filled circles come from the numerical simulations. σ_{yz} in the strong (weak) coupling limit is shown [dashed (dotted) line]. The numerical results are obtained with cluster perturbation theory for a cluster of size $N_c = 2^3$; the single-particle Hamiltonian has $m = 3/2$, $k_0 = 3\pi/8$.
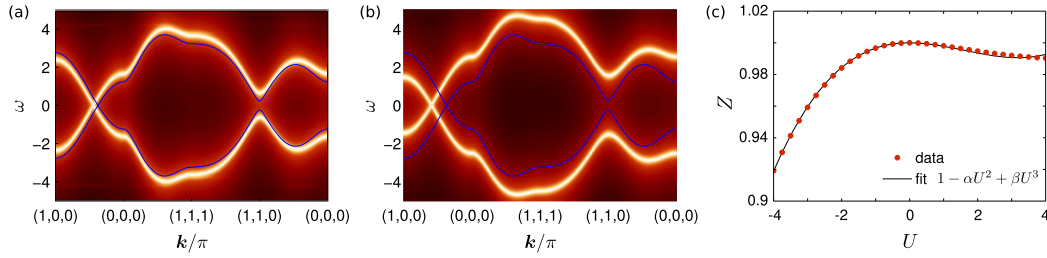
FIG. 2 (color online).   Density plot of the single particle spectral function $A(\omega, \boldsymbol{k})$ for (a) $U = 1$, (b) $U = 3$ obtained via CPT, shown on a logarithmic color scale. The noninteracting band structure (solid blue line) is the same as in Fig. 1. (c) Dependence of the residue Z of the Weyl quasiparticles on U; it is well approximated by a cubic polynomial.

instabilities [43] beyond a critical U) because they are located at special high-symmetry k points. The CPT calculation corroborates this. We thus need to turn on a finite ϵ to get nontrivial evolution. At $U = 0$, we find a total of 16 Weyl points when $|\epsilon| < 1$, setting $t = 1$. (Going from 8 to 16 Weyl points as ϵ is turned on does not violate the indivisible nature of Weyl points since the CDW changes the BZ.) When $\epsilon = 0$, four Weyl points occur at $k_z = 0$, while four other ones at π/a, where we have reinstated the spacing of the original cubic lattice a. When $0 < \epsilon < 1$, the eight nodes at $k_z = 0$ "split" to ones at $k_z a = \pm \sin^{-1}(\epsilon/2)$, similarly for $k_z = \pi/a$. A finite U moves the eight nodes nearest to $k_z = 0$ towards (away from) $k_z = 0$ since a repulsive (attractive) U disfavors (favors) the charge imbalance. This is confirmed by Fig. 3, which shows $\mathcal{H}_t$ obtained using CPT.

Long-ranged Coulomb interaction.—We have so far limited our discussion to short-ranged interactions. However, in an electronic WSM the screening of the Coulomb interaction is weak due to the vanishing density of states at the Fermi energy. Using RPA, it was shown [27] that for linearly dispersing electrons in three dimensions interacting via an instantaneous Coulomb $1/r$ repulsion, the quasiparticle at the node $\boldsymbol{k}_0$ is marginally destroyed: $\mathrm{Im}\Sigma_R(\omega + i0^+, \boldsymbol{k}_0) \sim |\omega|$, resulting in a "marginal Weyl liquid." Notwithstanding, this does not alter the fundamental Berry curvature structure around the (marginal) Weyl point. Indeed, let us consider the low-energy description near such an isotropic point: $\mathcal{H}_t(\boldsymbol{k}) = -G(0, \boldsymbol{k})^{-1} = f(k)\boldsymbol{k} \cdot \boldsymbol{\sigma}$, where $f = 1 + \lambda \ln(\Lambda/k)$ [27]. Crucially, the
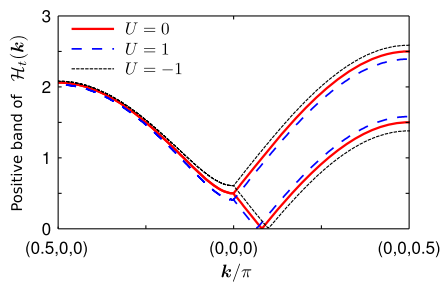

FIG. 3 (color online).   Positive band of the topological Hamiltonian $\mathcal{H}_t$ of model II ($\epsilon = 0.5$) with varying Hubbard U along a cut through the BZ. $U = 0$ is the noninteracting band structure.

Berry curvature $\nabla \times \mathcal{A}$ is independent of the overall real renormalization factor f as it measures the *complex phase* of the G eigenstates as they are parallel transported in the BZ. Thus, the Berry flux through a small sphere surrounding the Weyl point will measure the same monopole charge as when $f \equiv 1$. An analogous statement can be made about the π Berry phase of the Dirac points of graphene in the presence of Coulomb repulsion.

Orthogonal Weyl semimetals.—We present a case where the above characterization of a Weyl-like liquid using $\mathcal{H}_t$ breaks down. The idea being that particular interactions can induce a phase where the charge carrying quasiparticles have the properties of a WSM but are *orthogonal* to the electron due to fractionalization. Such a phase admits a simple and stable slave-particle description: the electron operator $c_{r,\sigma}$ can be written as the product $f_{r,\sigma}\tau_r^x$ of a slave fermion $f_{r,\sigma}$ carrying the *charge* (and spin), and a slave Ising pseudospin τ_r^x. A $\mathbb{Z}_2$ gauge redundancy emerges because of the decomposition. In terms of these slave operators, a WSM results when the f fermions form a WSM while the pseudospins are ordered. However, if they become disordered, an orthogonal WSM results for the electrons: The f fermions constitute a Weyl liquid since the pseudospins and $\mathbb{Z}_2$ gauge field are gapped, but they are orthogonal to the electrons (the electronic quasiparticle weight vanishes). The resulting orthogonal WSM is a cousin phase of the orthogonal metal [28]. It has qualitatively the same thermodynamic and transport [44,45] properties as a Weyl liquid: T^3 heat capacity, quantum oscillations [17], and AQH response. However, the electron Green's function G shows a hard "Mott" gap, thus no Weyl points. In this sense, the AQH response can no longer be obtained using $\mathcal{H}_t = -G(0, \boldsymbol{k})^{-1}$. Instead, one has to use the f-fermion Green's function. We thus have an instance where the adiabaticity relation to bare electrons breaks down, but where the topological Hamiltonian approach can be adapted by identifying the low-energy excitations. A similar situation will arise for other orthogonal states, such as orthogonal topological insulators [46].

Conclusion.—We have shown how to characterize interacting WSMs via the many-body Berry curvature (derived from the zero-frequency Green's function) allowing the identification of the monopole structure of the Weyl points.

We have argued that the existence of quasiparticles is not necessary in this; for example, the latter are marginally destroyed in a WSM with long-ranged Coulomb repulsion. As a natural extension, we note that $\mathcal{H}_t$ can also be used to efficiently identify Weyl nodes lying away from the Fermi surface, for example, in a doped Weyl semimetal, which proves much simpler than resolving the full spectral function. In closing, our work shows the importance of the Berry connection derived from the Green's function in the study of correlated fermions, especially their robust (quasi)topological features, in the gapless regime. We have illustrated that these ideas can be implemented numerically to study realistic models.

[1] A. K. Geim and K. S. Novoselov, Nat. Mater. **6**, 183 (2007).

[2] A. H. Castro Neto, F. Guinea, N. M. R. Peres, K. S. Novoselov, and A. K. Geim, Rev. Mod. Phys. **81**, 109 (2009).

[3] M. Z. Hasan and C. L. Kane, Rev. Mod. Phys. **82**, 3045 (2010).

[4] X.-L. Qi and S.-C. Zhang, Rev. Mod. Phys. **83**, 1057 (2011).

[5] X. Wan, A. M. Turner, A. Vishwanath, and S. Y. Savrasov, Phys. Rev. B **83**, 205101 (2011).

[6] G. Xu, H. Weng, Z. Wang, X. Dai, and Z. Fang, Phys. Rev. Lett. **107**, 186806 (2011).

[7] W. Witczak-Krempa and Y. B. Kim, Phys. Rev. B **85**, 045124 (2012).

[8] W. Witczak-Krempa, G. Chen, Y. B. Kim, and L. Balents, Annu. Rev. Condens. Matter Phys. **5**, 57 (2014).

[9] A. A. Burkov and L. Balents, Phys. Rev. Lett. **107**, 127205 (2011).

[10] H. B. Nielsen and M. Ninomiya, Phys. Lett. **130B**, 389 (1983).

[11] F. D. M. Haldane, Phys. Rev. Lett. **93**, 206602 (2004).

[12] K.-Y. Yang, Y.-M. Lu, and Y. Ran, Phys. Rev. B **84**, 075129 (2011).

[13] A. M. Turner and A. Vishwanath, arXiv:1301.0330.

[14] O. Vafek and A. Vishwanath, Annu. Rev. Condens. Matter Phys. **5**, 83 (2014).

[15] S. A. Parameswaran, T. Grover, D. A. Abanin, D. A. Pesin, and A. Vishwanath, Phys. Rev. X **4**, 031035 (2014).

[16] P. Hosur, Phys. Rev. B **86**, 195102 (2012).

[17] A. C. Potter, I. Kimchi, and A. Vishwanath, arXiv:1402.6342.

[18] I. Panfilov, A. A. Burkov, and D. A. Pesin, Phys. Rev. B **89**, 245103 (2014).

[19] G. A. Volovik, The Universe in a Helium Droplet (Oxford University Press, New York, 2003).

[20] A. Go, W. Witczak-Krempa, G. S. Jeon, K. Park, and Y. B. Kim, Phys. Rev. Lett. **109**, 066401 (2012).

[21] Z. Wang and S.-C. Zhang, Phys. Rev. B **86**, 165116 (2012).

[22] V. Mastropietro, arXiv:1310.5638.

[23] A. Sekine and K. Nomura, J. Phys. Soc. Jpn. **83**, 094710 (2014).

[24] This notation was introduced in Ref. [25] in the context of interacting topological insulators. We keep it, although we deal with gapless systems. This is motivated because the topological Hamiltonian captures the Berry phase properties of the electrons (such as hedgehogs).

[25] Z. Wang and B. Yan, J. Phys. Condens. Matter **25**, 155601 (2013).

[26] D. Sénéchal, D. Perez, and M. Pioro-Ladrière, Phys. Rev. Lett. **84**, 522 (2000).

[27] A. A. Abrikosov and S. D. Beneslavskii, JETP **32**, 699 (1971).

[28] R. Nandkishore, M. A. Metlitski, and T. Senthil, Phys. Rev. B **86**, 045128 (2012).

[29] Z. Wang, X.-L. Qi, and S.-C. Zhang, Phys. Rev. B **85**, 165126 (2012).

[30] Z. Wang and S.-C. Zhang, Phys. Rev. X **2**, 031008 (2012).

[31] H.-H. Hung, L. Wang, Z.-C. Gu, and G. A. Fiete, Phys. Rev. B **87**, 121113 (2013).

[32] T. C. Lang, A. M. Essin, V. Gurarie, and S. Wessel, Phys. Rev. B **87**, 205101 (2013).

[33] X. Deng, K. Haule, and G. Kotliar, Phys. Rev. Lett. **111**, 176404 (2013).

[34] M. Laubach, J. Reuther, R. Thomale, and S. Rachel, arXiv:1312.2934.

[35] F. Grandi, F. Manghi, O. Corradini, C. M. Bertoni, and A. Bonini, arXiv:1404.1287.

[36] C. Fang, M. J. Gilbert, X. Dai, and B. A. Bernevig, Phys. Rev. Lett. **108**, 266802 (2012).

[37] H. So, Prog. Theor. Phys. **74**, 585 (1985).

[38] K. Ishikawa and T. Matsuyama, Z. Phys. C **33**, 41 (1986).

[39] See Supplemental Material at http://link.aps.org/supplemental/10.1103/PhysRevLett.113.136402, which includes Refs. [40–42] for text, with equations and figures, providing detailed support for the statements made in the article.

[40] S. Engelsberg and J. R. Schrieffer, Phys. Rev. **131**, 993 (1963).

[41] G. Mahan, Many-Particle Physics, Physics of Solids and Liquids (Springer, New York, 2000).

[42] S. Das Sarma, E. H. Hwang, and W.-K. Tse, Phys. Rev. B **75**, 121406 (2007).

[43] J. Maciejko and R. Nandkishore, Phys. Rev. B **90**, 035126 (2014).

[44] P. Hosur and X. Qi, C.R. Phys. **14**, 857 (2013).

[45] R. Lundgren, P. Laurell, and G. A. Fiete, arXiv:1407.1435.

[46] J. Maciejko, V. Chua, and G. A. Fiete, Phys. Rev. Lett. **112**, 016404 (2014).